European Polymer Journal 44 (2008) 3213–3221

Contents lists available at ScienceDirect

European Polymer Journal

journal homepage: www.elsevier.com/locate/europolj

Novel rheological features of molten SEBS copolymers: Mechanical relaxation at low frequencies and flow split

Alfonso Arevalillo [a], María Eugenia Muñoz [a], Anton Santamaría [a,*], Luisa Fraga [b], Juan Antonio Barrio [b]

[a] Polymer Science and Technology Department and Polymer Institute POLYMAT, Faculty of Chemistry, University of the Basque Country UPV/EHU, P.O. Box 1072, 20080 San Sebastián, Spain
[b] Technology Centre REPSOL YPF, Road N-V, km 8, 28931 Móstoles, Madrid, Spain

ARTICLE INFO

Article history:
Received 13 March 2008
Received in revised form 23 June 2008
Accepted 9 July 2008
Available online 25 July 2008

Keywords:
SEBS
Rheology
Mechanical relaxation
Cylinder alignment
Flow split
Entanglements

ABSTRACT

Poly(styrene)-poly(ethylene-co-butylene)-poly(styrene) (SEBS) triblock copolymers with a PS volume fraction $\phi = 0.30$ are investigated. The analysis of the loss tangent at low frequencies leads to define a mechanical relaxation associated to the blocking effect of ordered PS cylinders on PEB chains motion. Submitting SEBS to a shear flow at 250 °C an orientation of the cylinders is observed. The effect of the molecular weight and the cylinder alignment on the relaxation is studied. Continuous flow experiments, in torsion and capillary mode, reveal the presence of very severe surface cracks which cause the phenomenon called "flow split". The correlation between dynamic viscoelastic results and flow split is investigated, concluding that this is related to an entanglement–disentenglement process, rather to an alignment effect of PS cylinders.

1. Introduction

The present study concerns morphological and rheological aspects of poly(styrene)-poly(ethylene-co-butylene)-poly(styrene) (SEBS) triblock copolymers. At low temperatures, the polystyrene chains constitute glassy domains, whereas the poly(ethylene-co-butylene) midblock chains form bridges between PS end blocks, causing an ordered network. This ordered, or microphase-separated state, can be typically arranged in spherical, cylindrical or lamellar structures. Only at high temperatures, well above the glass transition temperature of PS, a disordered state is reached giving rise to a liquid which shows the typical viscoelastic response of a homogeneous polymer melt in the terminal zone. Therefore, the ordered and disordered states (separated by the order–disorder transition temperature, ODT) are characterized by qualitative different low-frequency rheological features, as has been shown in the literature for different block copolymers [1–12]. Among the works devoted to elucidating the relationship between morphology and rheology of block copolymers, we remark the outstanding paper of Kossuth et al. [13] which schematically shows the respective viscoelastic responses of cubic, hexagonal and lamellar phases. All the investigations analyse the behaviour of the elastic (G′) and viscous (G″) moduli, comparing the response of homogeneous melts (disordered state) to that of ordered or micro-phase separated state.

The effect of flow fields on the orientation of block copolymers structures in the melt has deserved certain attention in the last 15 years. We dare to recommend two papers: the feature article of Wiesner on order and dynamics of diblock copolymers under large amplitude oscillatory flow [14] and the review paper of Hamley [15] on the use of strong shear fields, large extensional flows and large-amplitude oscillatory shear to align lamellar, hexagonal and cubic micellar morphologies of AB diblock

* Corresponding author. Tel.: +34 943 018184; fax: +34 943 015270.
E-mail address: antxon.santamaria@ehu.es (A. Santamaría).

0014-3057/$ - see front matter © 2008 Elsevier Ltd. All rights reserved.
doi:10.1016/j.eurpolymj.2008.07.028

and ABA triblock type copolymers. Hamley also refers to the rheological and thermodynamical properties of aligned samples, which depend on the extent of alignment. Mesophase order of morphologies, induced by flow fields, is also considered in more recent papers [16–18]. The particular effect of extrusion flow to align the PS cylinders of a SBS copolymer was first studied by Keller et al. [19]. More recently, extrusion flows involving different shear rates have been used to orient the micro-phases of different multiblock polymers and, eventually, to destroy this orientation [20–22].

In this paper we investigate no-sheared and sheared SEBS samples, offering an original rheological perspective based on the behaviour of the loss tangent at low frequencies, which allows us to define a mechanical relaxation associated to the presence of ordered micro-domains. Continuous flow experiments, in torsion and capillary mode, are also contemplated, revealing the presence of very severe surface cracks leading to the phenomenon called "flow split". The correlation between dynamic viscoelastic results and flow split is investigated.

2. Experimental

The investigated triblock copolymer is an experimental SEBS synthesized by Repsol-YPF, which has a weight average molecular weight M_w = 75,000 g/mol, a polydispersity index of 1.2 and a PS volume fraction ϕ = 0.30. The (weight) fractions of 1–2 PB and 1–4 PB were, respectively, 0.38 and 0.33. Another SEBS copolymer of the same chemical composition and molecular weight M_w = 55,000 g/mol is also considered for comparison purposes.

The viscoelastic behaviour of compression moulded (T = 190 °C and 200 kg/cm^2) samples was investigated using a ARG2 rheometer with a parallel-plate fixture (25 mm diameter) to conduct oscillatory frequency sweep experiments in the linear regime. The same apparatus was employed to study the effect of a continuous shear flow field on SEBS, following a protocol which is limited by the rheological response of the sample: (a) Shear rate increase from 0.1 to 0.6 s^{-1} in 120 s. (b) Constant shear rate 0.6 s^{-1} during 300 s. The selected temperature (T = 250 °C) and shear flow conditions are critical, since at higher temperatures the low viscosity leads to centrifugal effects and at lower temperatures severe flow instabilities (in particular flow split) occur. Frequency sweep experiments were carried out immediately after shearing process was properly accomplished. Measurements were also conducted after different resting times to analyse the recovery of the sample after shearing. The measurements were carried out in nitrogen atmosphere; time sweep experiments of G′ and G″ (not shown) were performed, leading us to discard any symptom of degradation in the samples.

Extrusion flow experiments were performed in a Göttfert 2002 rheometer using a capillary die of dimensions R = 0.5 mm and L/D = 30/1, at temperatures and shear rates indicated in Section 3.

Microphotographs and rheological results shown below, clearly indicate that at the temperatures considered in this work (230–250 °C) the sample is in an ordered state, that is to say below the order–disorder temperature T_{ODT}. Actually, according to our own thermorheological results (not displayed here), which coincide with results taken from literature for SEBS with the same PS content [23], the order–disorder temperature is higher than 300 °C. The sound thermodynamic analysis reported by Bates [24] for block copolymers constituted by blocks of chemical dissimilarity resembling our SEBS copolymers, leads us to assume that a PS volume fraction of ϕ = 0.30, such as that of our samples, gives rise to a hexagonal morphology. Although TEM is not the best method to observe the morphology of block copolymers, because of the eventually spurious effect of microtoming, microphotographs (Fig. 1) of quenched samples compressed at 250 °C, hint a hexagonal arrangement of PS cylinders. These appear dark, caused by RuO_4 staining, whereas PEB matrix is bright. TEM microphotographs of samples quenched after shearing in the rheometer were also obtained to investigate the morphological changes.

3. Results and discussion

3.1. Dynamic viscoelastic behaviour: the observation of a mechanical relaxation at low frequencies

Fig. 2 shows the dynamic viscoelastic behaviour of the investigated SEBS (M_w = 75,000 g/mol) sample in the region of low frequencies. As reported for other block copolymers at temperatures $T < T_{ODT}$, the presence of ordered microstructures alters the terminal viscoelastic zone. Instead of the dependences $G' \propto \omega^2$ and $G'' \propto \omega$, with $G'' > G'$, observed for homogeneous melts (including disordered block copolymers), a predominantly elastic response ($G' > G''$), with $G' \propto \omega^{0.25}$ and $G'' \propto \omega^{0.7}$ at the lowest frequencies, is noticed in the ordered state (Fig. 2). This result, obtained with a sample which reveals a hexagonal arrangement, practically coincides with the power law frequency dependence of the elastic modulus presented by Kossuth et al. [13] for the same arrangement. In their schematic of the relationship between G′ and the low frequency

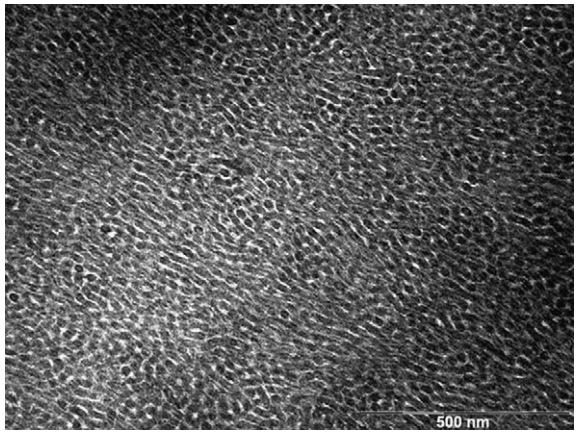

Fig. 1. TEM microphotographs of quenched samples compressed at 250 °C. Hexagonal arrangement of PS cylinders appears dark, whereas PEB matrix is bright.

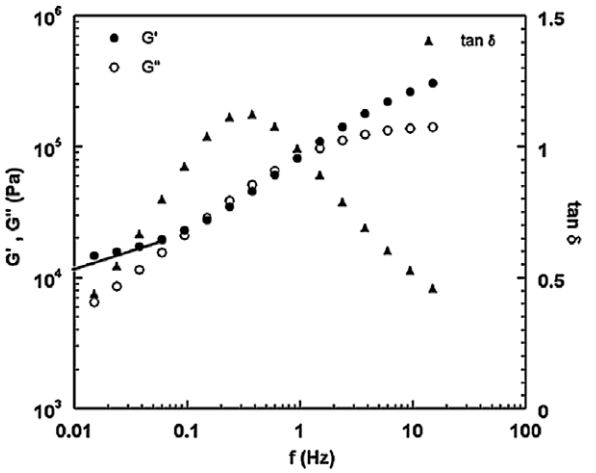

Fig. 2. Dynamic viscoelastic functions for SEBS (M_w = 75,000 g/mol) sample at T = 250 °C Storage and loss moduli and loss tangent as a function of frequency. The line corresponds to the scaling law proposed by Kossuth et al. [13] for systems with a hexagonal phase (see text).

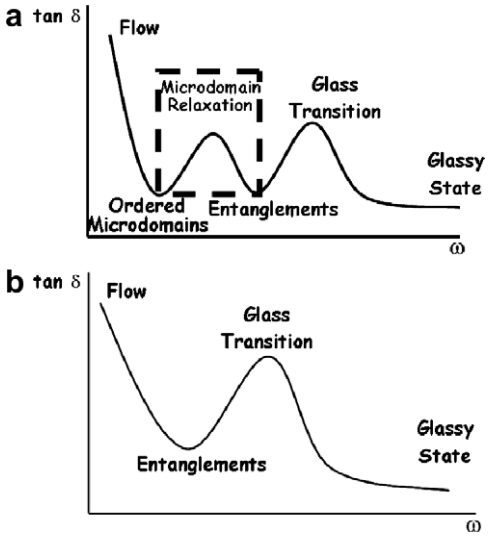

Fig. 3. General trend of the loss tangent as a function of frequency. (a) Adaptation of the viscoelastic pattern of ordered block copolymers, envisaged by Kossuth et al. [13] (see text). (b) Viscoelastic spectrum of a homogeneous polymer melt.

behaviour, these authors report respective G' $\propto \omega^{0.3}$ and G′ $\propto \omega^{0.5}$ dependences for systems with hexagonal and lamellar phases and G′ independent of frequency for cubic arrangement.

Although the presence of a low frequency tan δ maximum, as such noticed in Fig. 2, has been reported in the literature for diblock copolymers by Zhang and Wiesner [12] and Wiesner [14] and triblock copolymers by Ryu et al. [25] and Brown et al. [26], it has not been interpreted in terms of chain dynamics. However, the physical interpretation of the dynamic viscoelastic results of block copolymers in the low frequency domain may be extended contemplating this mechanical relaxation. As for the recently investigated polymer nanocomposites by Fernández et al. [27], the transition represents the hindering effect of a structure (ordered microdomains, in the case of block copolymers) to the mobility of the chain associated to flow. In the disordered state ($T > T_{ODT}$) ordered microdomains disappear and chains are free to move: then tan $\delta \to \infty$ at low frequencies and the spectrum resembles that of homopolymers, with no secondary relaxation. Fig. 3 shows the difference between the tan δ spectrum of a melt copolymer which contains ordered microdomains and a homogeneous copolymer melt (disordered state). Fig. 3a is actually an adaptation of the viscoelastic pattern of ordered block copolymers, envisaged by Kossuth et al. [13], whereas Fig. 3b is the viscoelastic spectrum of an amorphous polymer, as depicted, for instance, by Ferry [28]. In homogeneous systems, as frequency decreases the loss tangent passes through a minimum separating motions within entanglement strands and motions across entanglement loci. In the case of triblock copolymer melts at $T < T_{ODT}$, a double constraint to motion is suffered by midblock flexible chains: (a) Chain entanglements (provided that the molecular weight of midblock polymer is higher than its entanglement molecular weight (M_e). (b) Chain bridging between end blocks, which results in interconnected microdomains.

According to this picture, the low tan δ values envisioned at high frequencies in Fig. 2 account for the entanglement effect, since the molecular weight of PEB midblock of our SEBS is far above its critical molecular weight for entanglements (M_e) which has been reported to be 2000 g/mol [29]. On the other hand, as frequency is decreased, the observed tan δ maximum marks a limit in the mobility of flexible chains in an ordered system. What is detected is the blocking effect of PS cylinders on PEB flexible chains motion. The characteristic time λ of the relaxation process is defined taking the inverse of the frequency ω_{max} at which $(\tan\delta)_{max}$ takes place: $\lambda = 1/\omega_{max}$. At a given temperature, the chain mobility that requires times larger than λ, which corresponds to the low frequency zone with respect to the maximum, is hindered. On the contrary, the chain mobility level involving times shorter than λ, corresponding to the high frequency zone is not obstructed. Considering the aforementioned double constraints undergone by PEB midblock chains, we can state that entanglement slippage motions are accomplished (because take place at $t < \lambda$). But, however, motions that imply distances larger than the strands between microdomains require times $t > \lambda$ and are blocked, as can be noticed by the tan δ decrease as frequency decreases (Fig. 2). Therefore, the relaxation time λ accounts for the blocking effect of the hexagonal morphology of our SEBS copolymer, consisted of cylindrical microdomains of the PS block in the matrix of the PEB block. The physical basis of our interpretation lies also in the model offered recently by Somma et al. [30] to explain that at high frequencies there is not appreciable effect of superimposed flow on viscoelastic results of molten polymers, whereas at low frequencies this background flow has a clear impact on the moduli. These authors recall that at any oscillation frequency ω only the motion modes with a characteristic relaxation time higher than $\tau = 1/\omega$ are excited, which

implies that at low frequencies the slower modes (those more affected by superimposed flow) are tested.

The effect of the molecular weight on the investigated relaxation is contemplated in Fig. 4. With the frequency range covered by our rheometer different parts of the spectrum are accessible, depending on the molecular weight of the polymer. In Fig. 4 it is seen that the secondary relaxation, $(\tan\delta)_{max}$, shifts to higher frequencies as the molecular weight decreases. This is a consequence of the displacement to high frequencies of the minimum associated to entanglements: in fact, this minimum (which is depicted in the general picture offered in Fig. 3) is out of the investigated frequency range for M_w = 55,000 g/mol and M_w = 75,000 g/mol samples. As a result of the shift of the spectrum, the blocking effect of the microdomains is noticed at shorter times (higher frequencies) as the length of the midblock chains is reduced. Our results indicate that the selected SEBS (M_w = 75,000 g/mol) is the most appropriate to investigate the rheological changes associated to the application of a flow field, a subject which is treated below.

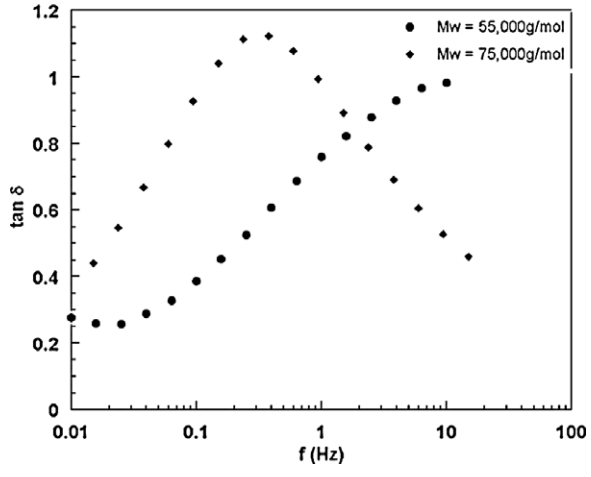

Fig. 4. Loss tangent as a function of frequency at T = 250 °C for SEBS samples of different molecular weights (● M_w = 55,000 g/mol, ♦ M_w = 75,000 g/mol).

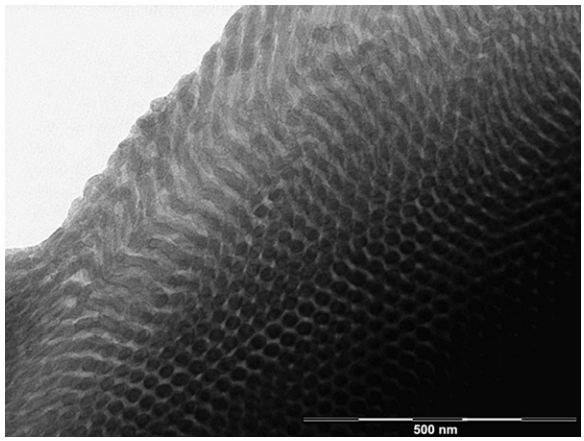

Fig. 5. TEM micrographs of a sheared SEBS (M_w = 75,000 g/mol) sample quenched after continuous torsion flow (see Section 2). Flow direction is normal to the picture. A misalignment is observed in the edge of the sample (upper left part).

3.2. Analysis of the rheological effects of alignment induced by shear flow and subsequent recovery

The morphological effect of the continuous shear flow, described in the Experimental Part, on SEBS (M_w = 75,000 g/mol) sample is shown in Fig. 5. Notwithstanding TEM is not as conclusive as two dimensional (2D)-SAXS, which has been successfully employed in oriented block copolymers [14,21,31–34], it can be deduced that cylindrical microdomains are aligned by the flow, although an orientation re-arrangement is noticed close to the edge. A meaningful difference is found between the dynamic viscoelastic response of the no-sheared sample and the sample which has been submitted to shear flow (Fig. 6). Oscillatory flow measurements were performed immediately after cessation of flow, so as the orientation shown in Fig. 5 is maintained. The behaviour changes from an elastic dominant response ($G' > G''$), observed for no-sheared sample, to $G'' > G'$ noticed for sheared sample (Fig. 6a). The results are analogous to those observed for shear-aligned polymer–silicate nanocomposites [35]. As for the low frequency secondary relaxation, $\tan\delta$ maximum, shown in Fig. 6b, a considerably shift to low frequencies is remarked for the sheared sample. It follows from this result that the characteristic relaxation time $\lambda = 1/\omega_{max}$ increases significantly as PS cylinders are aligned: This signifies that the blocking effect of the cylinders is reduced. We recall that complete motion of the midblock chains is hindered by hexagonal packing; only the chain mobility level involving times shorter than λ is not obstructed. The increase in relaxation time λ indicates that larger PEB midblock chain strands are implicated in motion when PS cylinders are aligned by flow. This also explains the high dissipation level (high $\tan\delta$ values, as $G'' > G'$) observed at low frequencies in the case of the sheared (aligned cylindrical microdomains) sample.

Rheological measurements carried out at different resting times after shear flow is ceased, reveal that cylinders orientation relaxes, although not completely. In Fig. 7 the evolution of the storage modulus and loss tangent with resting time is presented. As resting time increases, both viscoelastic functions tend to approach the behaviour reported for no-sheared SEBS. This result suggests a certain recovery from a flow oriented cylindrical phase towards a non-oriented PS cylinders morphology, but 2D-SAXS experiments, which are out of the scope of this paper, would be necessary to confirm completely this hypothesis. The recovery process is analysed in Fig. 8 which shows the evolution with time of a characteristic parameter, the relaxation time $\lambda = 1/\omega_{max}$. The rheological data suggest that the sample tends to the corresponding initial morphology of the no-sheared state. However, the value characteristic of the no-sheared SEBS at 250 °C, λ = 2.7 s, is not reached. Moreover, our data show a saturation of the recovery, since λ levels off after 60 min. This incomplete recovery indicates that the initial equilibrium conditions

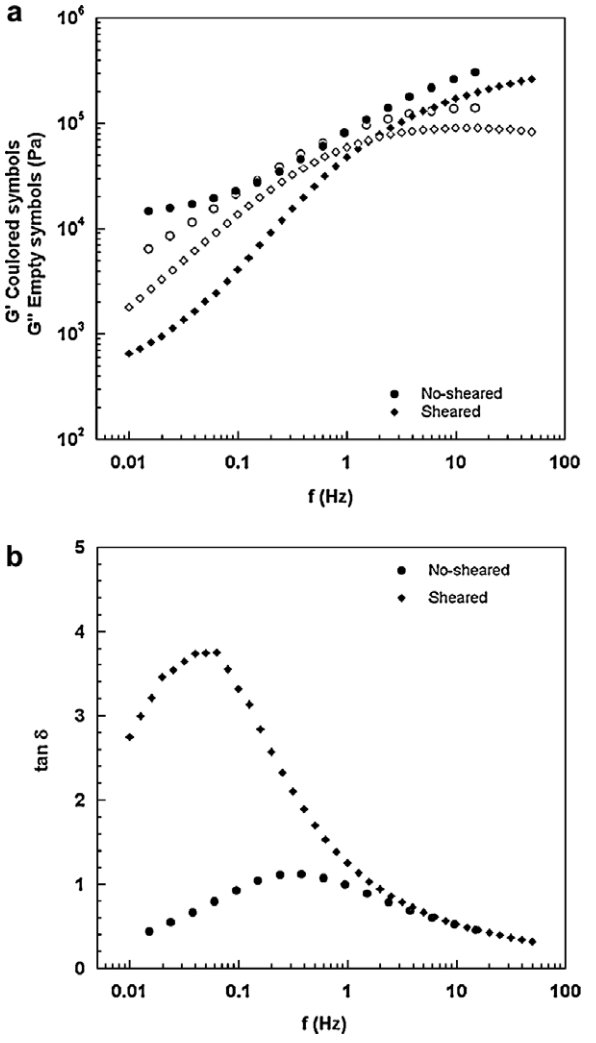

Fig. 6. Dynamic viscoelastic functions of the no-sheared and sheared SEBS (M_w = 75,000 g/mol) sample (see Fig. 5); (a) Storage and loss moduli as a function of frequency; (b) Loss tangent as a function of frequency.

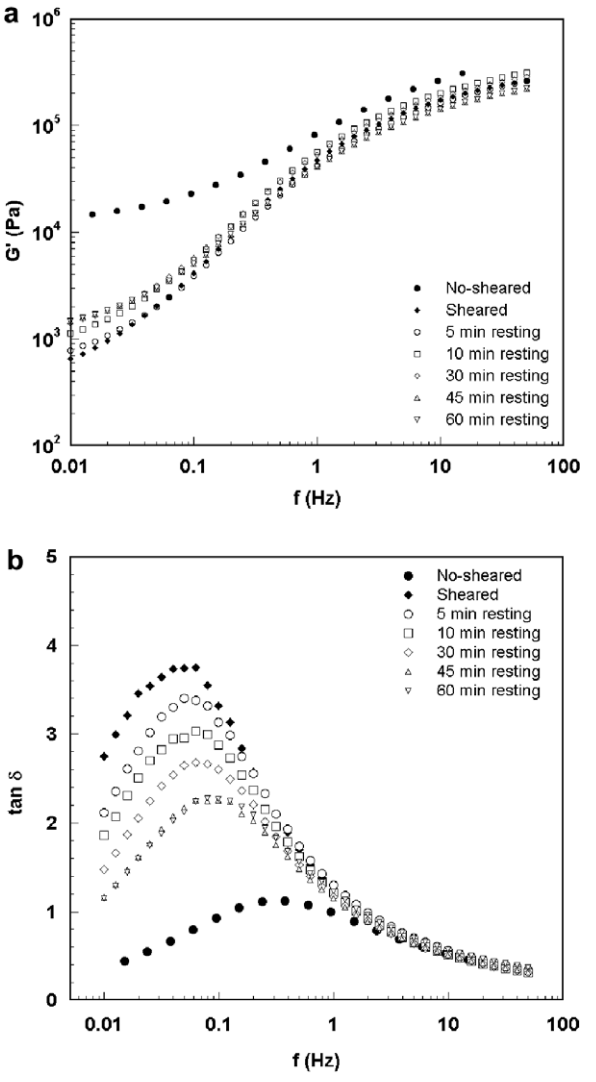

Fig. 7. Dynamic viscoelastic functions for SEBS (M_w = 75,000 g/mol) sample at T = 250 °C taken at the indicated resting times after shear is ceased. (a) Storage modulus; (b) Loss tangent. Notwithstanding the long resting times analysed, the response of the no-sheared sample is not attained.

are not recovered after cessation of flow. It may be suggested an anchoring effect of the rheometer plate, creating a new equilibrium state which is not destabilized at 250 °C.

The problems derived from continuous flow instabilities, mentioned in the Experimental Part, lead us to investigate the potential effect of cylinders alignment on the onset of flow split.

3.3. Very severe surface cracking: flow split in parallel plate flow and capillary flow

A striking flow distortion phenomenon is presented in Fig. 9: during plate–plate continuous (not oscillatory) torsion flow the initial disc sample splits in several arms. Needles to say the splitting process is accompanied by a torque reduction with time. This phenomenon has been probably already seen by other researchers when dealing with cone–plate or plate–plate experiments, but to our knowledge such severe fracture has not been reported in the literature. In a paper published by Hutton in *Nature* in 1963 [36] the flow instability which is currently termed "edge fracture" is described and a viscoelastic explanation of its origin is given. The phenomenon initiates as an indentation at the periphery of the sample and grows radially inwards in a cone–plate or parallel-plate rheometer. Hutton demonstrated that liquids can fracture in shear, provided that the total elastic energy contained in the sheared sample exceeds a critical value. In marked contrast with the extensively studied capillary flow instabilities, the analysis of flow instabilities in cone–plate or parallel flow is much more reduced: In our opinion Ref. [37–45] constitute outstanding contributions. Considering the soundest explanation offered in the literature, we assume that propagation and growth of peripheral cracks radially inward would lead

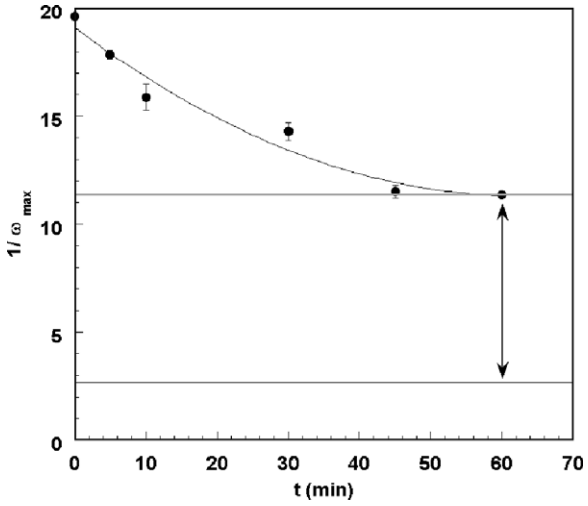

Fig. 8. Evolution of the characteristic relaxation time $\lambda = 1/\omega_{Max}$ as resting time increases. The parallel to the axis low line marks the value of λ for no-sheared sample. A part of the process is, therefore, irreversible.

to the split of the disc in several arms observed in Fig. 9. The phenomenon (which can be called "torsion flow split") resembles another striking case of very severe instability firstly reported by one of the authors [46]: The scission of ethane/propylene molten copolymer extrudates into two branches at the die exit in capillary flow. This "capillary flow split" has also been reported for polybutadiene [47] and SEBS copolymers [48,49]. Notwithstanding the stimulating contribution of Santanach et al. to unveil the phenomenon, the conditions for the occurrence of flow split at the capillary exit remain unclear. In any case, both phenomena, torsion flow split and flow split at the capillary exit, should be considered as very severe cases of surface cracking. In capillary flow, cracks are produced due to an elongational acceleration of the melt surface after it exits the die, whereas in torsion flows fracture occurs whenever the first normal stress difference N_1 [36,37] or the second normal stress difference N_2 [38–40], exceed a critical value. The occurrence of capillary flow split in our SEBS samples is shown in Fig. 10. Summaries of torsion flow split results and capillary flow split results are presented, respectively, in Tables 1 and 2.

Interestingly, Santanach et al. [48] observe capillary flow split for SEBS copolymers forming hexagonal-packed cylinders of PS, but not for SEBS forming spherical microphases. The authors verify that only for the latter SEBS the loss modulus G'' overtakes the storage modulus G', which is a symptom of less melt elasticity. Looking upon this result, we contemplate an analysis of the eventual correlation between oscillatory flow results and flow split. As it is seen in Fig. 6a the oscillatory flow behaviour changes from an elastic dominant response ($G' > G''$), observed for the original (no-sheared) sample, to $G'' > G'$ noticed for the sheared sample constituted by flow aligned PS cylinders. Continuous flow experiments at different temperatures and shear rates were performed with both samples in order to notice differences in torsion flow split. The results are included in Table 1. No significant difference is noted between sheared and no-sheared samples, stemming doubts on the effect of cylinder alignment on torsion flow split results. Two aspects should be considered to try to disclose the origin of the observed flow split: (a) Actual misalignment of PS cylinders in the plate touching surface of the sample (edge in Fig. 5). (b) Similar dynamic viscoelastic behaviour for no-sheared and shear-aligned samples at high frequencies (Fig. 6b), close to the characteristic entanglements minimum.

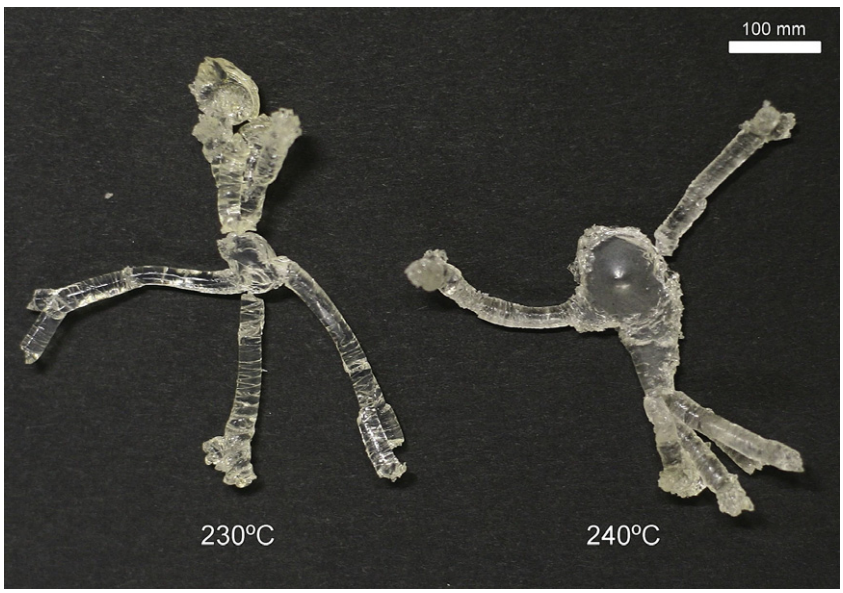

Fig. 9. Torsion flow split (see text) observed for SEBS (M_w = 75,000 g/mol) sample at the indicated temperatures and $\dot{\gamma} = 0.6\ s^{-1}$. Results obtained for all the samples under different conditions are summarized in Table 1.

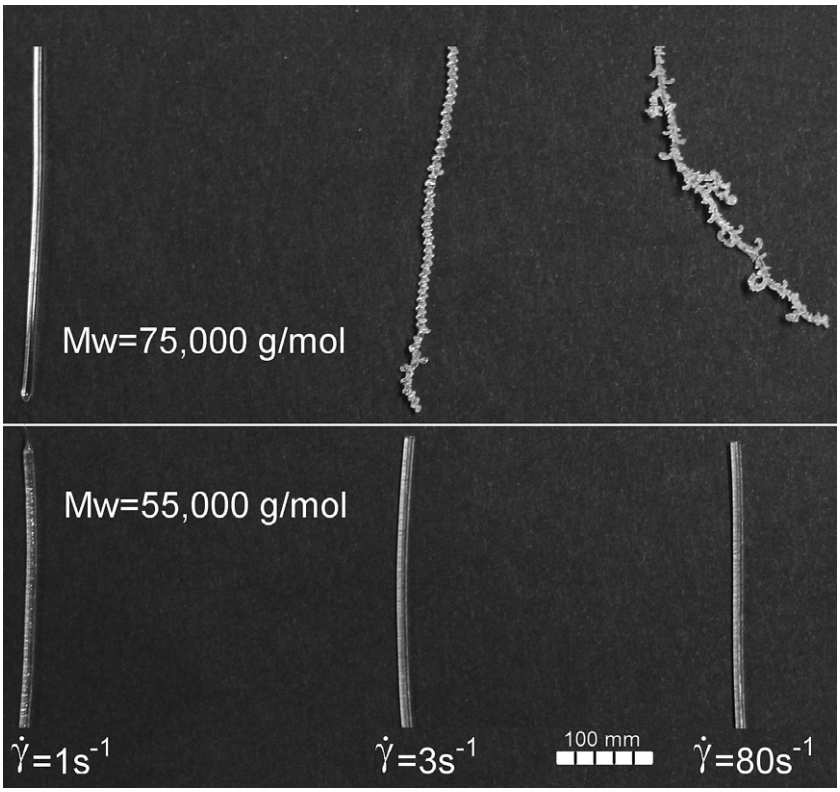

Fig. 10. SEBS (M_w = 75,000 g/mol) (top) and SEBS (M_w = 55,000 g/mol) (bottom) extrudates obtained at 250 °C and the indicated shear rates. A severe sharkskin leading to an incipient flow split is observed for SEBS (M_w = 75,000 g/mol) sample at $\dot{\gamma} = 3\,s^{-1}$. Flow split is observed for the same sample at $\dot{\gamma} = 80\ \ s^{-1}$. Results are summarized in Table 2.

Table 1
Continuous torsion flow results at the indicated temperatures and shear rates

	T = 250 °C	T = 245 °C	T = 240 °C	T = 230 °C
No sheared SEBS (M_w = 75,000 g/mol)	Stable flow $\dot{\gamma} \leqslant 1 s^{-1}$, Torsion flow Split $\dot{\gamma} \geqslant 1.5\ s^{-1}$	Torsion flow split $\dot{\gamma} \geqslant 0.6\ s^{-1}$	Torsion flow split $\dot{\gamma} \geqslant 0.6\ s^{-1}$	Torsion flow split $\dot{\gamma} \geqslant 0.6\ s^{-1}$
Sheared SEBS (M_w = 75,000 g/mol)	Stable flow $\dot{\gamma} \leqslant 0.6\ s^{-1}$	Torsion flow split $\dot{\gamma} \geqslant 0.6\ s^{-1}$	Torsión flow split $\dot{\gamma} \geqslant 0.6\ s^{-1}$	Torsion flow split $\dot{\gamma} \geqslant 0.6\ s^{-1}$
No sheared SEBS (M_w = 55,000 g/mol)	Stable flow $\dot{\gamma} \leqslant 5\ s^{-1}$	Stable flow $\dot{\gamma} \leqslant 0.6\ s^{-1}$	Stable flow $\dot{\gamma} \leqslant 0.6\ s^{-1}$	Stable flow $\dot{\gamma} \leqslant 0.6\ s^{-1}$

High shear rate measurements were limited by centrifugal effects. Torsion flow split phenomenon is depicted in Fig. 9. SEBS (M_w = 75,000 g/mol) sample was sheared at 250 °C as explained in the experimental part and then the temperature was reduced to the indicated values to perform torsion flow experiments. Measurements at 250 °C were carried out after 5 min. and 30 min. resting times: no difference was found (see text and Fig. 7).

Table 2
Capillary flow results at 250 °C.

Simple	$\dot{\gamma} \leqslant 1.5\ s^{-1}$	$3.0 \geqslant \dot{\gamma} \leqslant 80\ s^{-1}$	$80 > \dot{\gamma} < 700\ s^{-1}$	$\dot{\gamma} \geqslant 700\ s^{-1}$
SEBS (M_w = 75,000 g/mol)	Smooth	Incipient capillary flow split	Capillary flow split	Capillary flow split
SEBS (M_w = 55,000 g/mol)	Smooth	Smooth	Sharkskin	Incipient capillary flow split

Capillary flow split phenomenon is depicted in Fig. 10.

Concerning point ***a***, to our knowledge only one published work relates the orientation of the microstructure to surface roughening (sharkskin) of multiblock copolymers. Phatak et al. [22] analyse die extrusion instabilities of lamellae forming triblock and pentablock copolymers composed of poly(cyclohexylethylene) and polyethylene. Certainly these authors do not report any flow split phenomenon, but they observe that sharkskin is much more severe in the pentablock copolymer. A double hypothesis is advanced: parallel alignment of triblock copolymer

lamellae near the die surface and shear induced disordering of pentablock copolymer lamellae in the vicinity of the slip layer. It is noteworthy that we have also observed a cylinder misalignment in the edge of our SEBS (M_w = 75,000 g/mol) sample (Fig. 5). However, we have not currently enough elements to establish a connection between the results of Phatak et al. and our own outcome.

On the other hand, referred to point ***b***, we have investigated the possible occurrence of flow instabilities in a low molecular weight SEBS (M_w = 55,000 g/mol) sample which displays a different dynamic response, as compared with SEBS (M_w = 75,000 g/mol) (Fig. 4). Since for the low molecular weight sample the loss factor minimum associated to entanglements is shifted to higher frequencies, only the blocking effect of microdomains (explained in Figs. 2–4) is noticed in the investigated frequency range. The attempts to look for flow split in this low molecular weight sample gives the results shown in Tables 1 and 2: no torsion flow split is observed and the inception of capillary flow split is shifted to very high shear rates. Then, a connection between dynamic viscoelastic response and flow split can be envisaged. Firstly, both no-sheared and sheared SEBS (M_w = 75,000 g/mol) samples, which reflect motions associated to entanglements (tan δ reduction at high frequencies observed in Fig. 6b), show flow split under very similar conditions (Table 1). On the contrary, flow split practically disappears for the low molecular weight sample (SEBS (M_w = 55,000 g/mol)) which does not depict any hint of entanglements in Fig. 4. We remark the similitude, in terms of experimental time ($t = 1/\omega$ or $t = 1/\dot{\gamma}$), between the investigated frequency and shear rate intervals. With these results in hand, we dare to assert that the very severe surface crack leading to flow split in our no-sheared and sheared SEBS (M_w = 75,000 g/mol) samples is related to an entanglement–disentanglement process, as that proposed by Wang [50], rather to an alignment effect of PS cylinders.

4. Conclusions

The mechanical relaxation, $(\tan\delta)_{max}$, observed for SEBS samples at low frequencies accounts for a hindering effect of the hexagonal packing of PS cylinder microdomains on PEB midblock flexible chains mobility. As the molecular weight is reduced, it is seen that the relaxation shifts to higher frequencies and the characteristic relaxation time $\lambda = 1/\omega_{Max}$ decreases. Therefore, the blocking effect of the microdomains is noticed at shorter times or higher frequencies as the length of the midblock chains decreases.

Submitting SEBS (M_w = 75,000 g/mol) to a continuous shear flow of 0.6 s^{-1} at 250 °C a cylinder alignment is provoked. The characteristic relaxation time λ is significantly larger for the sheared sample than for the no-sheared original sample. This indicates that larger strands of midblock chains would be involved in motion when the PS cylinders are aligned.

Measurements carried out at different resting times after shear flow is ceased, reveal that the alignment induced by flow is not stable. The evolution with time of the relaxation time λ suggests that the sheared sample tends to its initial equilibrium (no-sheared) state. However, our data show a saturation of the recovery after 45 min.

Continuous flow experiments, in torsion and capillary mode, reveal the presence of very severe surface cracks leading to the phenomena called torsion flow split and capillary flow split. Sheared and no-sheared SEBS (M_w = 75,000 g/mol) samples show practically identical flow split results. For both samples, in the upper part of the frequency interval investigated (similar in terms of time to the analysed shear rate range) the characteristic entanglements minimum is approached. In the case of SEBS (M_w = 55,000 g/mol) torsion and capillary flow split disappear and no hint of entanglements is observed in dynamic viscoelastic results, on the contrary to sheared and no-sheared SEBS (M_w = 75,000 g/mol) samples. This leads us to suggest flow split is related to an entanglement–disentanglement process, rather to an alignment effect of PS cylinders.

Acknowledgments

Financial support through MEC (MAT2007-62151) (Spanish Government) is acknowledged. The authors thank the University Juan Carlos I for TEM microphotographs and GIC 07/135-IT-284-07 (Basque Government).

References

[1] Chung CI, Gale JC. Newtonian behaviour of a styrene-butadiene-styrene block copolymer. J Polym Sci 1976;14(6):1149–56.
[2] Gouinlock EV, Porter RS. Linear dynamic mechanical properties of an SBS block copolymer. Polym Eng Sci 1977;17(8):534–42.
[3] Chung CI, Lin MI. Nature of melt rheological transition in a styrene-butadiene-styrene block copolymer. J Polym Sci, Polym Phys 1978;16(3):545–53.
[4] Cohen RE, Ramos AR. Homogeneous and heterogeneous blends of polybutadiene, polyisoprene, and corresponding diblock copolymers. Macromolecules 1979;12:131–4.
[5] Widmaier JM, Meyer GC. Structural evolution of an ABA poly(styrene-b-isoprene) block copolymer with temperature. J Polym Sci, Polym Phys 1980;18(11):2217–25.
[6] Cohen RE, Wilfong DE. Properties of block copolymers and homopolymer blends comprised of 1,2-polybutadiene and 1, 4-polybutadiene. Macromolecules 1982;15:370–5.
[7] Bates FS. Block copolymers near the microphase separation transition. 2. Linear dynamic mechanical properties. Macromolecules 1984;17:2607–13.
[8] Han CD, Kim J. Rheological technique for determining the order-disorder transition of block copolymers. J Polym Sci, Polym Phys 1987;25(8):1741–64.
[9] Han CD, Kim J, Kim JK. Determination of the order-disorder transition temperature of block copolymers. Macromolecules 1989;22:383–94.
[10] Rosedale JH, Bates FS. Rheology of ordered and disordered symmetric poly(ethylenepropylene)-poly(ethylethylene) diblock copolymers. Macromolecules 1990;23:2329–38.
[11] Bates FS, Rosedale JH, Fredrickson GH. Fluctuation effects in a symmetric diblock copolymer near the order–disorder transition. J Chem Phys 1990;92(10):6255–70.
[12] Zhang Y, Wiesner U. Rheology of lamellar polystyrene-block-polyisoprene diblock copolymers. Macromol Chem Phys 1998;199:1771–84.
[13] Kossuth MB, Morse DC, Bates FS. Viscoelastic behaviour of cubic phases in block copolymer melts. J Rheol 1999;43(1):167–96.
[14] Wiesner U. Lamellar diblock copolymers under large amplitude oscillatory shear flow: order and dynamics. Macromol Chem Phys 1997;198:3319–52.
[15] Hamley IW. Structure and flow behaviour of block copolymers. J Phys: Condens Matter 2001;13:R643–71.

[16] Kotaka T, Okamoto M, Kojima A, Kwon YK, Nojima S. Elongational flow-induced morphology change of block copolymers. 2. A polystyrene-block-poly(ethylene butylenes)-block-polystyrene triblock copolymer with cylindrical microdomains. Polymer 2001;42:3223–31.
[17] Mortensen K, Theunissen E, Kleppinger R, Almdal K, Reynaers H. Shear-induced morphologies of cubic ordered block copolymer micellar networks studied by in situ small-angle neutron scattering and rheology. Macromolecules 2002;35: 7773–81.
[18] Sebastian JM, Lai C, Graessley WW, Register RA, Marchand GR. Steady-shear rheology of block copolymer melts: zero-shear viscosity and shear disordering in body-centered-cubic systems. Macromolecules 2002;35:2700–6.
[19] Keller A, Pedemonte E, Wilmouth FM. Macro-lattice from segregated amorphous phases of a three block copolymer. Nature 1970;225(5232):538–9.
[20] Leist H, Geiger K, Wiesner U. Orientation flip of lamellar polystyrene–polyisoprene diblock copolymers under extrusion. Macromolecules 1999;32:1315–7.
[21] Geiger K, Knoll K, Langela M. Microstructure and rheological properties of triblock copolymers under extrusion conditions. Rheol Acta 2002;41:345–55.
[22] Phatak A, Macosko CW, Bates FS, Hahn SF. Extrusion of triblock and pentablock copolymers: evolution of bulk and surface morphology. J Rheol 2005;49(1):197–214.
[23] Kim JK, Jung DS, Kim J. Morphology and rheological behaviour of mixtures of poly(styrene-b-ethylene-co-butylene-styrene) block copolymer and poly(2,6-dimethyl-1,4-phenylene ether). Polymer 1993;34(22):4613–24.
[24] Bates FS. Polymer–polymer phase behaviour. Science 1991;251:898–904.
[25] Ryu CY, Lee MS, Hajduk DA, Lodge TP. Structure and viscoelasticity of matched asymmetric diblock and triblock copolymers in the cylinder and sphere microstructures. Polym Sci, Polym Phys 1997;35:2811–23.
[26] Brown K, Hooker JC, Creton C. Micromechanisms of tack of soft adhesives based on styrenic block copolymers. Macromol Mater Eng 2002;287:163–79.
[27] Fernández I, Santamaría A, Muñoz ME, Castell P. A rheological analysis of interactions in phenoxy/organoclay nanocomposites. Euro Polym J 2007;43:3171–6.
[28] Ferry JD. Viscoelastic properties of polymers. 3rd ed. New York: Wiley; 1980. p. 47.
[29] Garcia Franco CA, Harrington BA, Lohse DJ. Effect of shot-chain branching on the rheology of polyolefins. Macromolecules 2006;39:2710–7.
[30] Somma E, Valentino O, Titomanlio G, Lanniruberto G. Parallel superposition in entangled polydisperse polymer melts: experimental and theory. J Rheol 2007;51(5):987–1005.
[31] Zhang Y, Wiesner U, Yang Y, Pakula T, Spiess HW. Annealing effects on orientation in dynamically sheared diblock copolymers. Macromolecules 1996;29:5427–31.
[32] Maring D, Wiesner U. Threshold strain value for perpendicular orientation in dynamically sheared diblock copolymers. Macromolecules 1997;30:660–2.
[33] Langela M, Wiesner U, Spiess W, Wilhelm M. Microphase reorientation in block copolymer melts as detected via FT rheology and 2D SAXS. Macromolecules 2002;35:3198–204.
[34] Oelschlaeger C, Gutmann JS, Wolkenhauer M, Spiess HW, Knoll K, Wilhelm M. Kinetics of shear microphase orientation and reorientation in lamellar diblock and triblock copolymer melts as detected via FT-rheology and 2D-SAXS. Macromol Chem Phys 2007;208:1719–29.
[35] Giannelis EP, Krishnamoorti R, Manias E. Polymer–silicate nanocomposites: model systems for confined polymers and polymer brushes. Adv Polym Sci 1999;138:107–47.
[36] Hutton JF. Fracture of liquids in shear. Nature 1963;200:646–8.
[37] Hutton JF. The fracture of liquids in shear: the effects of size and shape. Proc R soc Lond A 1965;287:222–39.
[38] Tanner RI, Keentok M. Shear fracture in cone-plate rheometry. J Rheol 1983;27(1):47–57.
[39] Lee CS, Tripp BC, Magda JJ. Does N_1 or N_2 control the onset of edge fracture? Rheol Acta 1992;31:306–8.
[40] Magda JJ, Baek SG. Concentrated entangled and semidilute entangled polystyrene solutions and the second normal stress difference. Polymer 1994;36(6):1187–94.
[41] Aral BK, Kalyon DM. Effects of temperature and surface roughness on time-dependent development of wall slip in steady torsional flow of concentrated suspensions. J Rheol 1994;38(4):957–72.
[42] Keentok M, Xue SC. Edge fracture in cone-plate and parallel plate flows. Rheol Acta 1999;38:321–48.
[43] Chan TW, Baird DG. An evaluation of a squeeze flow rheometer for the rheological characterization of a filled polymer with a yield stress. Rheol Acta 2002;41:245–56.
[44] Schweizer Th. Comparing cone-partitioned plate and cone-standard plate shear rheometry of a polystyrene melt. J Rheol 2003;47(4):1071–85.
[45] Inn YW, Wissbrun KF, Denn MM. Effect of edge fracture on constant torque rheometry of entangled polymer solutions. Macromolecules 2005;38:9385–8.
[46] Fernández M, Santamaría A, Muñoz-Escalona A, Méndez L. A striking hydrodynamic phenomenon: split of a polymer melt in capillary flow. J Rheol 2001;45(2):595–602.
[47] Zhu Z. Wall slip and extrudate instability of 4-arm star polybutadienes in capillary flow. Rheol Acta 2004;43:373–82.
[48] Santanach Carreras E, El Kissi N, Piau JM. Exit delayed transversal primary cracks and longitudinal secondary cracks: extrudate splitting and continuous peeling. Block copolymer extrusion distortions. J Non-Newt Fluid Mech 2005;131:1–21.
[49] Piau JM, Santanach Carreras E, Suarez Dabo E. Continuous peeling extrusion of SEBS block copolymers. J Non-Newt Fluid Mech 2007;147:139–48.
[50] Wang SQ. A coherent description of nonlinear flow behaviour of entangled polymers as related to processing and numerical simulations. Macromol Mater Eng 2007;292:15–22.